NASA Technical Memorandum 81470

AN IMPROVED PREDICTION METHOD FOR THE NOISE GENERATED IN FLIGHT BY CIRCULAR JETS

James R. Stone and Francis J. Montegani
Lewis Research Center
Cleveland, Ohio

Prepared for the
Ninety-ninth Meeting of the Acoustical Society of America
Atlanta, Georgia, April 21-25, 1980

AN IMPROVED PREDICTION METHOD FOR THE NOISE GENERATED IN FLIGHT BY CIRCULAR JETS

by James R. Stone and Francis J. Montegani

National Aeronautics and Space Administration
Lewis Research Center
Cleveland, Ohio 44135

E-403

ABSTRACT

A semi-empirical model for predicting the noise generated by jets exhausting from circular nozzles is presented and compared with small-scale static and simulated-flight data. The present method is an updated version of that part of the original NASA Aircraft Noise Prediction Program (1974) relating to circular jet noise. The earlier method has been shown to agree reasonably well with experimental static and flight data for jet velocities up to ~520 m/sec. The poorer agreement at higher jet velocities appeared to be due primarily to the manner in which supersonic convection effects were formulated. The purely empirical supersonic convection formulation is replaced in the present method by one based on theoretical considerations. Other improvements of an empirical nature have been included based on model-jet/free-jet simulated-flight tests. The effects of nozzle size, jet velocity, jet temperature, and flight are included.

INTRODUCTION

Accurate noise prediction methods are now required in order to predict the environmental impact of airport operations on the surrounding communities, as well as for the realistic design of new aircraft and the development of noise reducing modifications to existing aircraft. The prediction method presented herein is an updated, more theoretically based, version of that part of the original NASA Aircraft Noise Prediction Program pertaining to circular nozzles (ref. 1). This paper deals only with the noise generated by the exhaust jet mixing with the surrounding air and does not consider other noises emanating from the engine such as narrow-band shock screech or internally-generated noises.

Although the numerous aspects of the mechanisms of jet noise generation are not fully understood, the necessity of predicting jet noise has led to the development of empirical procedures. The NASA interim prediction method for jet noise (ref. 1) and an updated Society of Automotive Engineers (SAE) method (ref. 2) are in current use. The SAE method shows reasonable agreement with static experimental data for jet velocities up to about 870 m/sec. The earlier NASA method (ref. 1) shows reasonable agreement with both static and flight data at jet velocities up to about 520 m/sec. However, at higher velocities and at locations near the jet axis (angles greater than about 130° with respect to the inlet) the noise is overpredicted. The poorer agreement at high jet velocities appeared to be due primarily to the manner in which supersonic convection effects were formulated. The highly empirical supersonic convection formulation of reference 1 is replaced by one (ref. 3) based on theoretical considerations (refs. 4 and 5). With these changes, the method presented herein agrees fairly well with the SAE method (ref. 2) under static conditions. The same relationships are then used to predict the noise in flight, in contrast to the SAE method, which uses a purely empirical approach for flight effects.

For supersonic jets not fully expanded to ambient pressure, shock/turbulence interaction noise must also be considered. The purely empirical shock noise procedure of reference 1 is replaced in the current method by a semi-empirical model based largely on the theory of Harper-Bourne and Fisher (ref. 6).

SYMBOLS

(All symbols are in SI units unless noted.)

A	area
c	speed of sound
D	nozzle diameter
F	functional relation (eq. (13))
f	1/3-octave-band center frequency
I	acoustic intensity
K_I	coefficient in equation (1)
k	ratio of convection velocity to jet velocity
ℓ	characteristic length
M	Mach number, V/c

n	convection factor exponent
ΘASPL	overall sound pressure level, dB re 20 $\mu N/m^2$
OASPL'	predicted OASPL uncorrected for refraction, dB re 20 $\mu N/m^2$
p	pressure
p_{ref}	reference pressure, 20 $\mu N/m^2$
$\overline{p^2}$	mean-square acoustic pressure fluctuation
R	source-to-observer distance
S	effective Strouhal number (eq. (12))
SPL	1/3-octave-band sound pressure level, dB re 20 $\mu N/m^2$
T	total temperature
V	velocity
X	source position downstream of nozzle exit plane
α	turbulent length scale ratio
β	effective angle of attack (fig. 1), deg
Δ	flight level relative to static, dB
ρ	density
θ	polar angle from inlet axis (fig. 1), deg
θ'	effective polar angle, $\theta(V_j/c_a)^{0.1}$, deg
θ_M	Mach angle, $\sin^{-1}(1/M_j)$, deg
ω	density exponent (eq. (4))

Subscripts:

a	ambient or apparent
c	convection
D	dynamic
e	effective
F	flight
ISA	international standard atmosphere (288 K and 101.3 kN/m^2)
j	fully-expanded jet

K	kinematic
S	static
So	source alteration
s	shock noise
90^o	parameter evaluated at $\theta = 90^o$
0	aircraft

FORMULATION OF PROCEDURE

The noise levels predicted are free-field (no reflections), far-field and lossless (i.e., the effects of atmospheric absorption are not included). The geometric variables describing the position of the observer relative to the engine are shown schematically in figure 1. The jet mixing noise and shock noise are assumed to by symmetric about the jet axis. The results of the prediction procedure are expressed in terms of SPL spectra at each angle of interest. (Acoustic power relations are not given explicitly, but power computations may be made by integrating the results numerically over all angles.)

The prediction is first developed for shock-free jet mixing noise with no flight effects. Then, the effects of flight are considered, and static-to-flight increments established. Finally, supersonic jet shock noise effects (static and flight) are incorporated into the prediction procedure.

Experimental noise measurements are often made at a distance far enough from the sources to be in the acoustic far field of each individual source, but not far enough away to treat the entire jet plume as a point source at the center of the nozzle exit plane. When such is the case, comparisons between experimental data and prediction must take source locations into account. The methods used to approximate these source location effects are given in appendix A.

Static Jet Mixing Noise

Lighthill's theoretical studies (refs. 7 and 8) established that the acoustic intensity of a shock-free jet varies with $\rho V_j^8 c_a^{-5} \ell^2$. If the characteristic dimension ℓ is taken to be the square root of the fully-expanded jet area A_j, the intensity I at a distance R from the source would be given at $\theta = 90^o$ by

$$I = K_I\left(\frac{\rho V_j^8 A_j}{c_a^5 R^2}\right) \tag{1}$$

where K_I is an experimentally determined coefficient.

In experiments, however, it is generally the mean-square pressure fluctuation $\overline{p^2}$ which is measured and not the intensity. This mean-square pressure fluctuation is given by $I\rho_a c_a$, so that

$$\overline{p^2} = K_I\left(\frac{\rho_a \rho V_j^8 A_j}{c_a^4 R^2}\right) \tag{2}$$

The mean-square pressure fluctuations are usually expressed in decibels (dB) referred to a reference pressure p_{ref}, and physical properties are often referred to those for the International Standard Atmosphere (ISA). Consequently, an equivalent relation to equation (2) can be written in dimensionless logarithmic terms:

$$\text{OASPL} = 10 \log\left(\frac{\overline{p^2}}{p_{ref}^2}\right) = 10 \log\left(\frac{K_I \rho_{ISA}^2 c_{ISA}^4}{p_{ref}^2}\right) + 10 \log\left(\frac{V_j}{c_a}\right)^8$$

$$+ 10 \log\left(\frac{A_j \rho_a \rho c_a^4}{R^2 \rho_{ISA}^2 c_{ISA}^4}\right) \tag{3}$$

Thus far in the present development, the characteristic density ρ has not been specified. Experimental results (e.g., ref. 9) indicate that at high jet velocities the noise increases with increasing jet density (decreasing jet temperature), approaching a square-law relation, $I \propto \rho_j^2$. On the other hand, at low jet velocity the noise decreases with increasing jet density, approaching an inverse relation, $I \propto \rho_j^{-1}$. These effects were incorporated into the earlier NASA prediction (ref. 1) by using the ambient density in equation (3) but adding a term $10 \log(\rho_j/\rho_a)^\omega$ to the right-hand side, where ρ_j is the fully-expanded

jet density. The following analytical expression for ω, developed in reference 1, will also be used herein,

$$\omega = \frac{3\left(\frac{V_j}{c_a}\right)^{3.5}}{0.6 + \left(\frac{V_j}{c_a}\right)^{3.5}} - 1 \tag{4}$$

This expression gives values similar to those recommended by the SAE procedure (ref. 2), as is shown in figure 2. The agreement is nearly exact over the range in which the SAE curve is based on experimental data. With this formulation for ω it was determined that the jet velocity exponent required adjustment to 7.5 from 8.0 to agree with data.

The effect of source convection on the noise radiation has been determined on theoretical grounds to introduce a directional effect on the noise level. According to Ffowcs Williams (ref. 4) the acoustic intensity is multiplied by the factor, $\left[\left(1 + M_c \cos\theta\right)^2 + \alpha^2 M_c^2\right]^{-n/2}$, where $M_c = kV_j/c_a$. In the present formulation the value of k is taken to be 0.62 and n is taken to be 3, as suggested by Goldstein and Howes (ref. 5). The value used for α is 0.2, essentially as determined by Larson, et al. (ref. 10). The resulting expression for OASPL uncorrected for refraction (OASPL') is given by

$$\mathrm{OASPL}' = 141 + 10\log\left[\left(\frac{\rho_a}{\rho_{ISA}}\right)^2\left(\frac{c_a}{c_{ISA}}\right)^4\right] + 10\log\left(\frac{A_j}{R^2}\right) + 10\log\left(\frac{\rho_j}{\rho_a}\right)^{\omega}$$

$$+ 10\log\left(\frac{V_j}{c_a}\right)^{7.5} - 15\log\left[\left(1 + M_c\cos\theta\right)^2 + \alpha^2 M_c^2\right] \tag{5}$$

(Note that for an ideal gas the term, $\left(\rho_a/\rho_{ISA}\right)^2\left(c_a/c_{ISA}\right)^4$, reduces simply to p_a^2/p_{ISA}^2.) The earlier NASA prediction (ref. 1) contained a more complicated jet velocity effect to give the experimentally observed trends at high jet velocity. This term is no longer needed with the theoretically more correct hand-

ling of supersonic convection. Corrections for the effects of refraction are incorporated in the spectral curves, as discussed in the following paragraph.

Spectral curves are shown in figure 3, where SPL-OASPL' is plotted at 10° increments as a function of the logarithm of the effective Strouhal number, S, where

$$S = \frac{fD}{V_j}\left(\frac{T_j}{T_a}\right)^{0.4(1+\cos\theta')} \tag{6}$$

where θ' is an effective angle given by $\theta\left(V_j/c_a\right)^{0.1}$, and D is the equivalent diameter based on fully-expanded jet area, $\sqrt{4A_j/\pi}$. These results are also given in table I for the convenience of the user. These curves were evolved through improvements to a similar set of curves determined empirically in reference 1. Integration of the spectral curves produces a difference between the corrected (OASPL) and uncorrected (OASPL') overall sound pressure levels, as indicated by the bottom row of table I. This difference is attributed to refraction.

In figure 4 the level of agreement between the present method and that of the SAE (ref. 2) over the range of the latter ($-0.4 \le \log(V_j/c_a) \le +0.4$ and $20^{\circ} \le \theta \le 160^{\circ}$) is illustrated. It can be seen that the general agreement is fairly good. Within this range, comparing at increments of 10° in θ and 0.05 in $\log(V_j/c_a)$, the standard deviation between the two methods is 1.8 dB.

Effects of Flight on Jet Mixing Noise

The effects of flight on jet mixing noise level are essentially as developed in reference 3, and the effect on frequency is treated in an analogous manner. In order to predict the effects of flight on jet mixing noise, three effects can be identified as follows:

$$OASPL_F - OASPL_S = \Delta_K + \Delta_D + \Delta_{So} \tag{7}$$

These effects are briefly summarized as follows:

(1) The kinematic effect, Δ_K, due to motion of the airplane with respect to the stationary observer.

(2) The dynamic effect, Δ_D, due to the motion of the sources with respect to the propagation medium.

(3) Source strength alteration, Δ_{S_O}, due to the effect of the reduced shear between the jet plume and the ambient air.

Kinematic effect. - There is general agreement in the literature on the calculation of Δ_K, that is:

$$\Delta_K = -10 \log\left[1 - M_o \cos(\theta + \beta)\right] \tag{8}$$

where M_o is the aircraft Mach number, V_o/c_a, and β is the effective engine angle of attack (fig. 1).

Dynamic effect. - As mentioned in developing the static prediction, source convection introduces a term, $\left[\left(1 + M_c \cos\theta\right)^2 + \alpha^2 M_c^2\right]^{-n/2}$. For an aircraft in motion, it was suggested by Ffowcs Williams (ref. 4) that M_c be replaced by $k(V_j - V_o)/c_a$. (As in the static case, $k = 0.62$, $n = 3$, and $\alpha = 0.2$.) Thus, the static to flight increment due to the dynamic effect becomes

$$\Delta_D = -15 \log\left\{\frac{\left[1 + k\left(\frac{V_j - V_o}{c_a}\right)\cos\theta\right]^2 + \alpha^2 k^2 \left(\frac{V_j - V_o}{c_a}\right)^2}{\left[1 + k\left(\frac{V_j}{c_a}\right)\cos\theta\right]^2 + \alpha^2 k^2 \left(\frac{V_j}{c_a}\right)^2}\right\} \tag{9}$$

This formulation is quite similar to one proposed by Cocking and Bryce (ref. 11), who used a relation of this type but with $k = 0.65$, $n = 3.8$, and $\alpha = 0.3$.

Source strength alteration. - The change in source strength in flight should be observable near $\theta = 90^o$, where the kinematic and dynamic effects are small. To correlate this effect, the approach is to replace the jet velocity, V_j, by an effective jet velocity, V_e, in equations (4) and (5). With this assumption, and deleting the convective te - which is small at $\theta = 90^o$ and is handled separately (eq. (9)) anyway, the OASPL at 90^o can be written as

$$OASPL_{90^\circ} = 141 + 10 \log\left[\left(\frac{\rho_a}{\rho_{ISA}}\right)^2 \left(\frac{c_a}{c_{ISA}}\right)^4\right] + 10 \log\left(\frac{A_j}{R^2}\right)$$

$$+ 10\omega \log\left(\frac{\rho_j}{\rho_a}\right) + 75 \log\left(\frac{V_e}{c_a}\right) \qquad (10)$$

where

$$\omega = \frac{3\left(\frac{V_e}{c_a}\right)^{3.5}}{0.6 + \left(\frac{V_e}{c_a}\right)^{3.5}} - 1 \qquad (10a)$$

As in the case of the static prediction, the jet velocity effect can be simplified from the earlier formulation (refs. 1 and 3) because of the improvement in modeling the supersonic convection effect. Analysis of recent free-jet simulated flight test results (e.g., refs. 12 and 13) indicates that the approximation, $V_e = V_j\left[1 - (V_o/V_j)\right]^{2/3}$, is appropriate. In terms of the static to flight increment, the resulting relation is

$$\Delta_{So} = 50 \log\left(1 - \frac{V_o}{V_j}\right) + 10\left\{\frac{3\left[\left(\frac{V_j}{c_a}\right)\left(1 - \frac{V_o}{V_j}\right)^{2/3}\right]^{3.5}}{0.6 + \left[\left(\frac{V_j}{c_a}\right)\left(1 - \frac{V_o}{V_j}\right)^{2/3}\right]^{3.5}} - \frac{3\left(\frac{V_j}{c_a}\right)^{3.5}}{0.6 + \left(\frac{V_j}{c_a}\right)^{3.5}}\right\} \log\left(\frac{\rho_j}{\rho_a}\right) \qquad (11)$$

Frequency shift. - The change in source motion from the static to the flight case also causes a Doppler shift in frequency. The formulation of this effect must take into account the fact that even in the static case, source motion is

present. The resulting expression for the nondimensional frequency parameter in flight is then as follows:

$$S = \frac{fD\left[1 - M_o \cos(\theta + \beta)\right]}{V_j\left(1 - \frac{V_o}{V_j}\right)}\left(\frac{T_j}{T_a}\right)^{0.4(1+\cos\theta')} \times \sqrt{\frac{\left[1 + \frac{k}{c_a}\left(V_j - V_o\right)\cos\theta\right]^2 + \frac{\alpha^2 k^2}{c_a^2}\left(V_j - V_o\right)^2}{\left(1 + \frac{kV_j}{c_a}\cos\theta\right)^2 + \alpha^2 k^2\left(\frac{V_j}{c_a}\right)^2}} \tag{12}$$

When $V_o = 0$, this expression reduces to equation (6).

Shock Noise

A theoretically-based model for the prediction of shock/turbulence interaction noise was developed by Harper-Borne and Fisher (ref. 6). Shock noise was found to increase with the parameter $\left(M_j^2 - 1\right)^2$, and this type of dependence was incorporated in the NASA Lewis prediction method (ref. 14). More recent experiments (ref. 15) have shown that this type of dependency is followed only to values of $\sqrt{M_j^2 - 1}$ slightly greater than 1.0, with noise levels changing little beyond this point. This effect is included in the present prediction by assuming

$$OASPL_s \propto 10 \log \frac{\left(M_j^2 - 1\right)^2}{1 + \left(M_j^2 - 1\right)^2}$$

The incorporation of the effects of flight, along with size, distance, and ambient condition corrections, leads to the following expression for the shock noise:

$$OASPL_s = 162 + 10 \log \left[\left(\frac{\rho_a}{\rho_{ISA}} \right)^2 \left(\frac{c_a}{c_{ISA}} \right)^4 \right] + 10 \log \left(\frac{A_j}{R^2} \right) + 10 \log \frac{\left(M_j^2 - 1 \right)^2}{1 + \left(M_j^2 - 1 \right)^2}$$

$$- 10 \log \left[1 - M_o \cos(\theta + \beta) \right] + F(\theta - \theta_M) \qquad (13)$$

where θ_M is the Mach angle given by $\sin^{-1}(1/M_j)$. The function F is given by

$$F = 0 \qquad \text{for } \theta \leq \theta_M \qquad (13a)$$

$$F = 0.75 \qquad \text{for } \theta > \theta_M$$

The appropriate nondimensional frequency parameter, again based on the Harper-Borne and Fisher (ref. 6) model, is given by

$$S_s = \left(\frac{fD}{kV_j} \right) \sqrt{M_j^2 - 1} \left[1 - M_o \cos(\theta + \beta) \right] \sqrt{\left[1 + k \left(\frac{V_j}{c_a} \right) \cos \theta \right]^2 + \alpha^2 k^2 \left(\frac{V_j}{c_a} \right)^2} \qquad (14)$$

Note that the convection velocity factor $k = 0.7$, instead of the 0.62 value appropriate for jet mixing noise, but the $\alpha = 0.2$ value is retained. The shock noise peaks at $S_s = 1.0$ and varies with $\log S_s$ as shown in figure 5 and tabulated in table II. The spectrum shape is significantly changed from that of reference 14, as indicated in figure 5.

COMPARISONS WITH EXPERIMENTAL DATA

This section contains a limited comparison of the present prediction method with experimental data obtained with model jets in anechoic facilities. Although there exists a great deal of additional experimental data with which comparisons may eventually be made, the present comparisons are considered to be sufficient to demonstrate the validity of the procedure.

Static Jet Mixing Noise

A rather comprehensive set of jet noise measurements was obtained by Tanna, et al. (ref. 16) in an anechoic facility. These results were shown to be free of contamination by extraneous noise sources and cover a wide range of jet conditions. These data have been generally accepted and have been used in validating other prediction procedures. Therefore, it seems appropriate to compare the present prediction method with this data set. The data were obtained for conical nozzles at subsonic conditions and convergent-divergent nozzles at the design point; the nozzle throat diameters were 5.08 cm. The data were reported on a lossless basis and are used herein on the same basis.

OASPL. - Overall sound pressure levels, corrected for size, distance, and properties are plotted against the jet velocity parameter, $\log(V_j/c_a)$, in figure 6 and compared with the present prediction. Such comparisons are shown for angles of 57° (fig. 6(a)), 86° (fig. 6(b)), 116° (fig. 6(c)), a 155° (fig. 6(d)). It appears that the effect of jet velocity is predicted reasonably over the range of these tests for nondimensional jet velocities, V_j/c_a, fr 0.35 to 2.55.

Further comparisons in terms of directivity over a [illegible] jet velocities ($0.8 \le V_j/c_a \le 2.55$) of interest for jet engines a[illegible]wn in figure 7. The effects of directivity are predicted reasonably well, although there is clearly an overprediction or a low measured level at the highest angle. For this rather limited data set, even including the highest angle, the standard deviation between the experimental data and the prediction is 1.6 dB with an average overprediction of less than 0.1 dB. (Excluding the highest angle, the standard deviation is reduced to 1.3 dB, and there is an average underprediction of 0.2 dB.)

Spectra. - Limited spectral comparisons are shown in figure 8 for the same conditions as the dir[illegible]vity comparisons of figure 7. Such comparisons are shown for angles of 57° (fig. 8(a)), 86° (fig. 8(b)), 116° (fig. 8(c)), and 155° (fig. 8(d)). The agreement generally appears to be good, but there may be some problems with the high-frequency experimental data, such as high SPL values resulting from electronic noise, dynamic range limitations, and large corrections for atmospheric absorption, as has been reported by others (e.g., ref. 17).

Jet Mixing Noise in Flight

The method presented herein was shown in reference 3 to predict the effect of flight on jet mixing noise to within a standard deviation of 1.5 dB for full-scale flight tests. It is shown in this section that this method also compares well with simulated-flight model-scale results. Limited comparisons are made with the experimental results of Kozlowski and Packman (ref. 17) for a 5.7-cm-diameter conical nozzle in a 0.91-m-diameter free jet in an anechoic chamber. Spectral comparisons are shown in figure 9 for a nondimensional jet velocity, V_j/c_a, of 1.38 and a free jet Mach number of 0.18. Comparisons are shown at angles, θ, of 65^o, 85^o, 115^o, and 148^o. The agreement is quite good, especially in the rear quadrant (115^o and 148^o) where jet noise is generally most dominant. The scatter at low frequencies for the experimental data at angles of 65^o and 85^o probably indicates the presence of some wall reflections, but for higher frequencies the agreement is excellent.

Shock Noise

Shock noise is present along with jet mixing noise for non-fully-expanded jets. For a given jet Mach number, shock noise increases relative to jet mixing as jet temperature is decreased. Therefore, comparisons at relatively low jet temperature (~394 K) are included. The experimental results are again from reference 17.

Static. - Comparisons at essentially static conditions ($M_0 = 0.03$) are shown in figure 10 for a jet Mach number of 1.41 and nondimensional jet velocities, V_j/c_a, of 1.38 (fig. 10(a)) and 1.63 (fig. 10(b)). Spectral comparisons with the jet-mixing and shock noise predictions, as well as total noise, are shown at angles, θ, of 65^o, 85^o, 115^o, and 148^o. As in figure 9, the low-frequency data at 65^o and 85^o appear to be influenced by reflections. In addition the high-frequency data show a "roll-up" at high frequencies which is thought to be anomalous. Although the shock noise prediction does not appear as accurate as the jet noise prediction, the effects of angle appear correct and the level and peak frequency are reasonably approximated.

Simulated flight. - Similar comparisons for essentially the same jet conditions as in figure 10 are shown in figure 11 for a free jet Mach number, M_0, of 0.18. By comparing figure 10(a) with figure 11(a) and figure 10(b) with figure 11(b), it can be seen that the effects of flight on level and frequency are predicted properly. It can also be seen that shock noise is predicted to be

more dominant in flight than under static conditions and this result is consistent with the experimental data. These figures also further illustrate the accuracy of the jet mixing noise prediction.

CONCLUDING REMARKS

An improved semi-empirical model for predicting the noise generated by jets exhausting from circular nozzles is presented and compared with small-scale static and simulated-flight data. The jet mixing noise prediction is developed largely from the theories of Goldstein (1973) and Ffowcs Williams (1963) along with some empirically determined elements. The theoretical basis for the shock noise model is from Harper-Bourne and Fisher (1973). The predictions formulated for both sources cover the full angular range from 0 to 180 degrees. There are no inherent limitations on the range of the prediction methods, and comparisons of the jet mixing noise model with experimental data are made at jet velocities from 120 to 880 m/sec.

The revised Society of Automotive Engineers (SAE) method is shown to agree reasonably well with the present jet mixing noise prediction in terms of static level, directivity, and spectra. The two methods agree within a 1.8-dB standard deviation in OASPL. Limited comparisons with model-scale simulated-flight data presented herein show that the levels and spectra are predicted accurately. An earlier report showed that this method predicts static to flight increments for full-scale jet mixing noise to within a 1.5-dB standard deviation in OASPL.

The shock noise method is shown to give reasonably accurate predictions statically and in flight, but detailed statistical comparisons have not been made.

APPENDIX A

SOURCE LOCATION CORRECTIONS

Experimental noise measurements are often made at a distance far enough away to be in the far field of any individual noise source region, but not far enough away to treat the entire exhaust plume as a point source at the center of the nozzle exit plane. When this is the case, the prediction for each source must take into account the location of that source. This appendix gives the methods used herein to approximate these source location effects. The geo-

metric relations for noise sources downstream of the nozzle exit are given in figure A1. The relationship of the actual source-to-observer distance, R, to its apparent value, R_a, for a source at a distance, X, downstream of the exit plane is as follows:

$$R = \sqrt{\left(R_a + X \cos \theta_a\right)^2 + X^2 \sin^2 \theta_a} \tag{A1}$$

The relationship of the actual angle, θ, to its apparent value, θ_a, is then

$$\theta = \sin^{-1}\left(\frac{R_a}{R} \sin \theta_a\right) \tag{A2}$$

Jet Mixing Noise

The relation for jet mixing noise source location is based very loosely on the data of reference 18. The approximate relation used is as follows:

$$X_j = \left(4 + \frac{\theta_a}{90^\circ}\right)D \tag{A3}$$

This is an approximation to the source position where the peak frequency noise at each angle is generated. The variation of source position with frequency is not given explicitly, but is included to some degree of approximation in the spectral shapes. Figure A2 shows the OASPL correction for distance and angle corrections for jet mixing noise as a function of apparent angle, θ_a, for various values of R_a/D.

Shock Noise

The relation used for shock/turbulence interaction noise source location has some foundation in the theory of Harper-Bourne and Fisher (ref. 6). Reference 6 indicates that the first shock occurs at $1.31\ D\sqrt{M_j^2 - 1}$ and that the spacing between shocks is about 6 percent of that distance. Furthermore, reference 6 indicates that about eight shocks are significant in the noise generation

process. The approximation used here emphasizes the earlier, stronger shocks and is given as follows:

$$X_s = 1.5\, D \sqrt{M_j^2 - 1} \qquad (A4)$$

REFERENCES

1. J. R. Stone, "Interim Prediction Method for Jet Noise," NASA TM X-71618 (1974).

2. "Gas Turbine Jet Exhaust Noise Prediction," Society of Automotive Engineers, SAE-ARP-876 (March 1978).

3. J. R. Stone, "An Improved Method for Predicting the Effects of Flight on Jet Mixing Noise," NASA TM-79155 (1979).

4. J. E. Ffowcs Williams, "The Noise from Turbulence Convected at High Speed. Phil. Trans. Roy. Soc. (London), Ser. A, 255, 469-503 (1963).

5. M. E. Goldstein and W. L. Howes, "New Aspects of Subsonic Jet Noise Theory," NASA TN D-7158 (1973).

6. M. Harper-Bourne and M. J. Fisher, "The Noise from Shock Waves in Supersonic Jets," in Noise Mechanisms AGARD-CPP-131, (Advisory Group for Aerospace Research and Development, Paris, 1973), pp. 11-1 to 11-13.

7. M. J. Lighthill, "On Sound Generated Aerodynamically. I. General Theory," Proc. Roy. Soc. (London), Ser. A., 211, 564-587 (1952).

8. M. J. Lighthill, "On Sound Generated Aerodynamically. II. Turbulence as a Source of Sound," Proc. Roy. Soc. (London), Ser. A, 222, 1-32 (1954).

9. R. G. Hoch, J. P. Duponchel, B. J. Cocking, and W. D. Bryce, "Studies of the Influence of Jet Density on Jet Noise," J. Sound Vib., 28, 649-668 (1973).

10. R. S. Larson, C. J. McColgan, and A. B. Packman, "Jet Noise Source Modification Due to Forward Flight," AIAA Paper No. 77-58 (January 1977).

11. B. J. Cocking and W. D. Bryce, "Subsonic Jet Noise in Flight Based on Some Recent Wing-Tunnel Tests," AIAA Paper No. 75-462 (March 1975).

12. K. K. Ahuja, B. J. Tester, and H. K. Tanna, "The Free Jet as a Simulator of Forward Velocity Effects on Jet Engine Noise," NASA CR-3056 (1978).

13. A. B. Packman and K. W. Ng, "Effects of Simulated Forward Flight on Subsonic Jet Exhaust Noise," AIAA Paper No. 75-869 (June 1975).

14. J. R. Stone, "An Empirical Model for Inverted-Velocity-Profile Jet Noise Prediction," NASA TM-73838 (1977).

15. J. M. Seiner and T. D. Norum, "Experiments on Shock Associated Noise of Supersonic Jets," AIAA Paper 79-1526 (July 1979).

16. H. K. Tanna, P. D. Dean, and R. H. Burrin, "The Generation and Radiation of Supersonic Jet Noise, Vol. III, Turbulent Mixing Noise Data," Final Rep. No. LG76ER0133-VOL-3, Lockheed-Georgia Co., Marietta, GA (1976). (AD-A032882, AFAPL-TR-76-65-VOL-3.)

17. H. Kozlowski and A. B. Packman, "Flight Effects on the Aerodynamic and Acoustic Characteristics of Inverted Profile Coannular Nozzles," NASA CR-3018 (1978).

18. C. L. Jaeck, "Static and Wind-Tunnel Near-Field/Far-Field Jet Noise Measurements from Model Scale Single-Flow Baseline and Suppressor Nozzles, Vol. I: Noise Source Locations and Extrapolation of Static Free-Field Jet Noise Data," Rep. No. D6-44121-1-VOL-1, Boeing Commercial Airplane Co., Seattle, WA (1976). (NASA CR-137913.)

TABLE I. - RECOMMENDED SPECTRA FOR JET MIXING NOISE

Frequency parameter, log S	Effective angle, θ', deg									
	0-110	120	130	140	150	160	170	180	190	200
	SPL-OASPL', dB									
-1.8	-39.1	-42.9	-44.0	-46.0	-44.4	-38.9	-35.8	-32.9	-29.6	-26.7
-1.7	-36.8	-40.5	-41.2	-42.8	-41.3	-34.4	-31.7	-29.1	-26.2	-23.7
-1.6	-34.5	-38.1	-38.4	-39.7	-38.2	-30.4	-28.0	-25.7	-23.2	-21.1
-1.5	-32.3	-35.7	-35.6	-36.5	-35.1	-26.8	-24.7	-22.7	-20.6	-18.8
-1.4	-30.0	-33.3	-32.8	-33.3	-31.9	-23.6	-21.8	-20.1	-18.3	-16.9
-1.3	-27.7	-30.9	-30.0	-30.2	-28.8	-20.8	-19.3	-17.8	-16.4	-15.4
-1.2	-25.4	-28.5	-27.2	-27.0	-25.6	-18.4	-17.1	-15.9	-14.9	-14.2
-1.1	-23.2	-26.1	-24.4	-23.9	-22.5	-16.3	-15.3	-14.4	-13.7	-13.4
-1.0	-21.1	-23.7	-21.6	-20.8	-19.5	-14.6	-13.9	-13.2	-12.9	-12.9
-.9	-19.1	-21.3	-18.8	-17.6	-16.7	-13.3	-12.8	-12.4	-12.4	-13.4
-.8	-17.4	-19.0	-16.2	-14.7	-14.1	-12.4	-12.0	-11.9	-12.9	-14.4
-.7	-15.9	-16.7	-14.1	-12.8	-11.9	-11.7	-11.5	-12.4	-13.9	-16.3
-.6	-14.7	-14.6	-12.5	-11.5	-10.3	-11.2	-12.0	-13.4	-15.8	-18.4
-.5	-13.7	-12.7	-11.2	-10.9	-9.7	-11.7	-13.0	-15.3	-17.9	-20.5
-.4	-12.8	-11.4	-10.6	-10.6	-10.3	-12.7	-14.8	-17.4	-20.0	-22.6
-.3	-12.1	-10.7	-10.3	-10.9	-11.7	-14.5	-16.8	-19.5	-22.1	-24.7
-.2	-11.6	-10.4	-10.6	-11.4	-13.6	-16.4	-18.8	-21.6	-24.2	-26.8
-.1	-11.3	-10.7	-11.2	-12.4	-15.4	-18.3	-20.8	-23.7	-26.3	-28.9
0	-11.1	-11.1	-12.4	-13.9	-17.2	-20.2	-22.8	-25.8	-28.4	-31.0
.1	-11.2	-11.6	-13.7	-15.5	-19.0	-22.1	-24.8	-27.9	-30.5	-33.1
.2	-11.3	-12.3	-15.0	-17.1	-20.8	-24.0	-26.8	-30.0	-32.6	-35.2
.3	-11.7	-13.2	-16.3	-18.7	-22.6	-25.9	-28.8	-32.1	-34.7	-37.3
.4	-12.3	-14.2	-17.6	-20.3	-24.3	-27.8	-30.8	-34.2	-36.8	-39.4
.5	-13.0	-15.2	-19.0	-21.9	-26.1	-29.7	-32.8	-36.3	-38.9	-41.5
.6	-13.7	-16.3	-20.3	-23.6	-27.9	-31.6	-34.8	-38.4	-41.0	-43.6
.7	-14.6	-17.4	-21.7	-25.2	-29.7	-33.5	-36.8	-40.5	-43.1	-45.7
.8	-15.6	-18.5	-23.0	-26.8	-31.5	-35.4	-38.8	-42.6	-45.2	-47.8
.9	-16.7	-19.7	-24.4	-28.4	-33.3	-37.3	-40.8	-44.7	-47.3	-49.9
1.0	-17.8	-20.9	-25.7	-30.0	-35.1	-39.2	-42.8	-46.8	-49.4	-52.0
1.1	-18.9	-22.1	-27.1	-31.6	-36.9	-41.1	-44.8	-48.9	-51.5	-54.1
1.2	-20.1	-23.3	-28.5	-33.2	-38.7	-43.0	-46.8	-51.0	-53.6	-56.2
1.3	-21.3	-24.5	-29.8	-34.8	-40.5	-44.9	-48.8	-53.1	-55.7	-58.3
1.4	-22.4	-25.7	-31.2	-36.4	-42.3	-46.8	-50.8	-55.2	-57.8	-60.4
1.5	-23.6	-26.9	-32.5	-38.0	-44.0	-48.7	-52.8	-57.3	-59.9	-62.5
1.6	-24.8	-28.1	-33.8	-39.6	-45.8	-50.6	-54.8	-59.4	-62.0	-64.6
1.7	-26.0	-29.3	-35.1	-41.2	-47.6	-52.5	-56.8	-61.5	-64.1	-66.7
1.8	-27.2	-30.5	-36.5	-42.8	-49.4	-54.4	-58.8	-63.6	-66.2	-68.8
OASPL-OASPL'	0.0	-0.5	-1.0	-1.5	-2.0	-2.5	-3.0	-3.5	-4.0	-4.5

TABLE II. - RECOMMENDED SPECTRUM FOR SHOCK NOISE

Frequency parameter, $\log S_s$	Relative level, SPL-OASPL, dB	Frequency parameter, $\log S_s$	Relative level, SPL-OASPL, dB
-1.8	-94.6	.1	-8.6
-1.7	-89.6	.2	-9.6
-1.6	-84.6	.3	-10.6
-1.5	-79.6	.4	-11.6
-1.4	-74.6	.5	-12.6
-1.3	-69.6	.6	-13.6
-1.2	-64.6	.7	-14.6
-1.1	-59.6	.8	-15.6
-1.0	-54.6	.9	-16.6
-.9	-49.6	1.0	-17.6
-.8	-44.6	1.1	-18.6
-.7	-39.6	1.2	-19.6
-.6	-34.6	1.3	-20.6
-.5	-29.6	1.4	-21.6
-.4	-24.6	1.5	-22.6
-.3	-19.6	1.6	-23.6
-.2	-14.6	1.7	-24.6
-.1	-9.6	1.8	-25.6
0	-7.6		

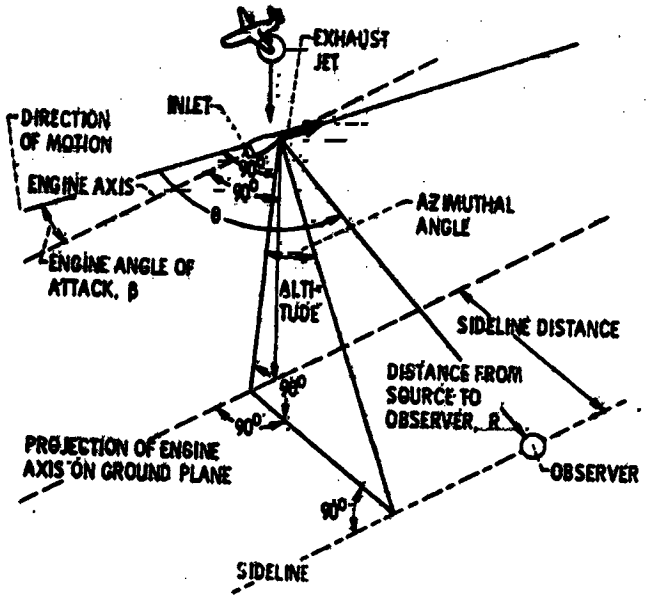

Figure 1. - Geometric variables describing position of airplane jet noise source with respect to an observation point.

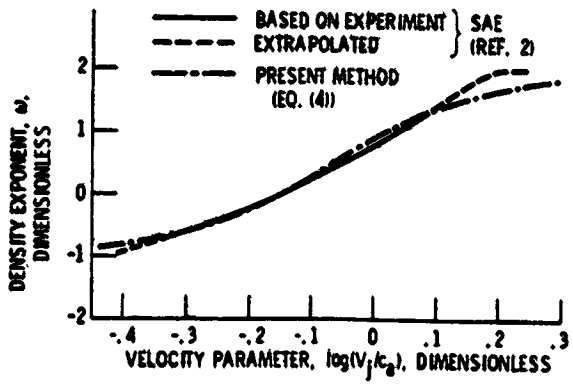

Figure 2. - Jet density exponent as a function of jet velocity parameter and comparison with SAE method (ref. 2).

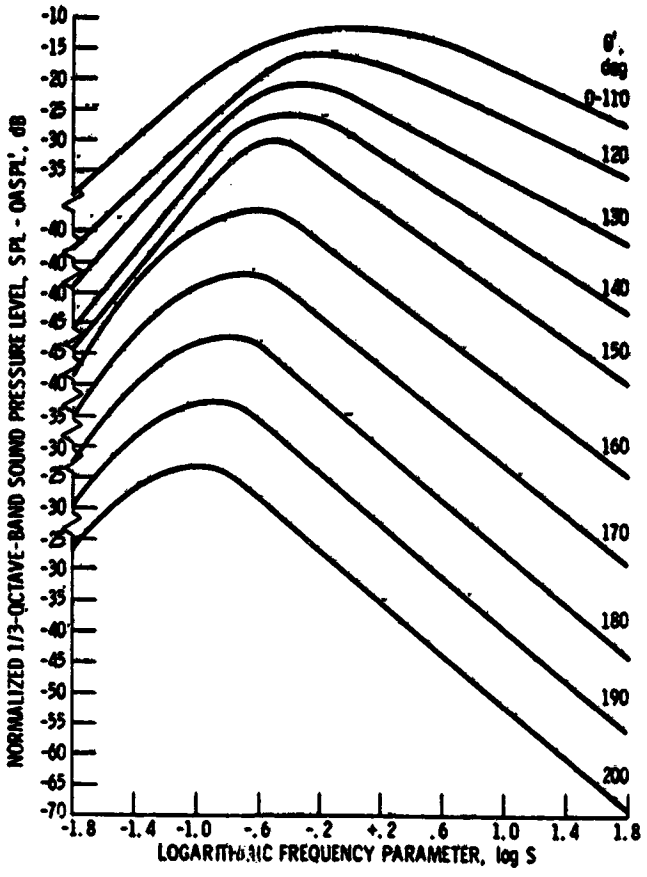

Figure 3. - Recommended spectra for jet mixing noise.

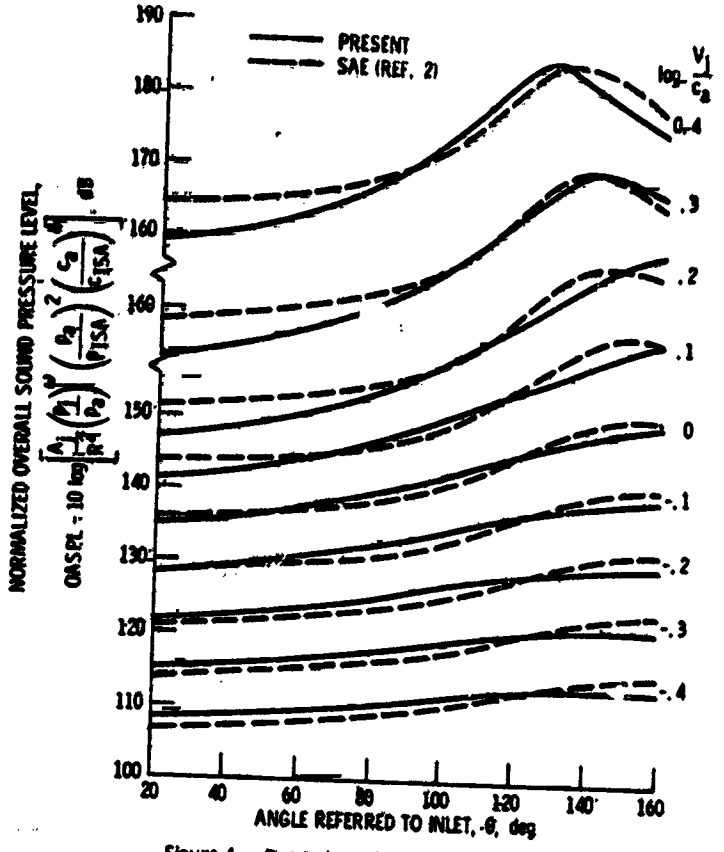

Figure 4. - Comparison of jet mixing noise directivity of present prediction with that of the SAE (ref. 2).

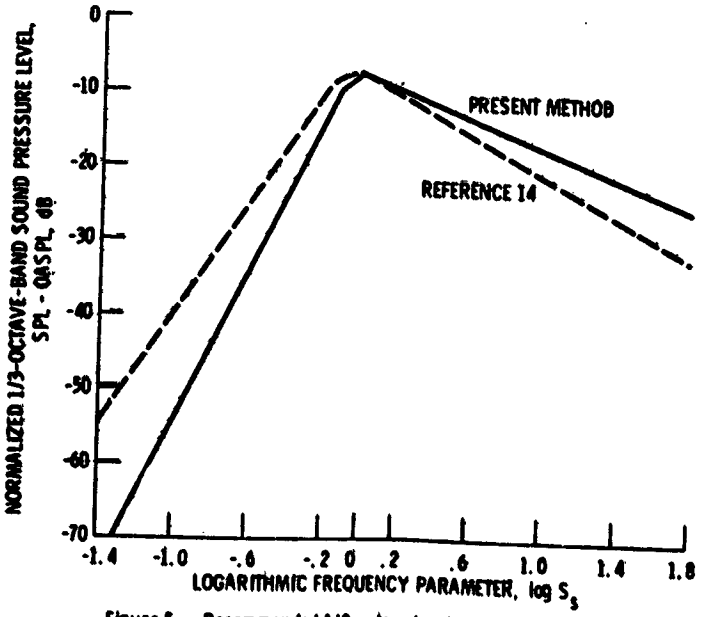

Figure 5. - Recommended 1/3-octave band spectrum for shock noise.

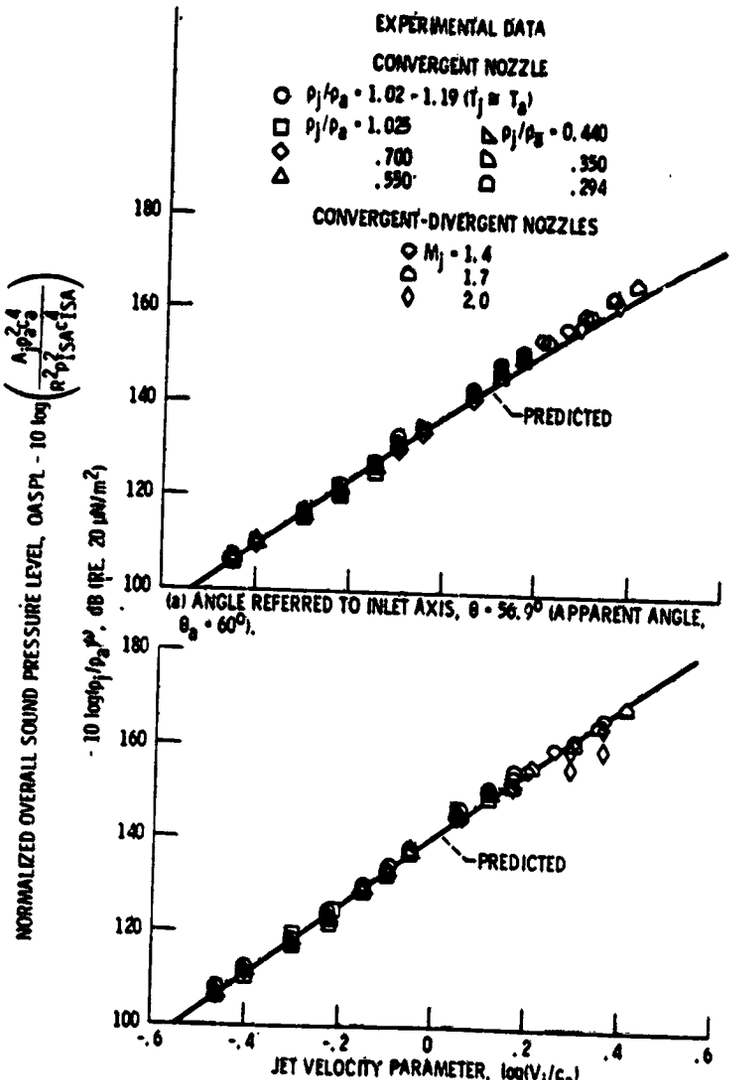

(a) ANGLE REFERRED TO INLET AXIS, θ = 56.9° (APPARENT ANGLE, θ_a = 60°).

(b) ANGLE REFERRED TO INLET AXIS, θ = 86.0° (APPARENT ANGLE, θ_a = 90°).

Figure 6. - Comparison of static jet mixing noise prediction with experimental OASPL data of Tanna, et al. (ref. 16) for 5.08-cm-diameter nozzles.

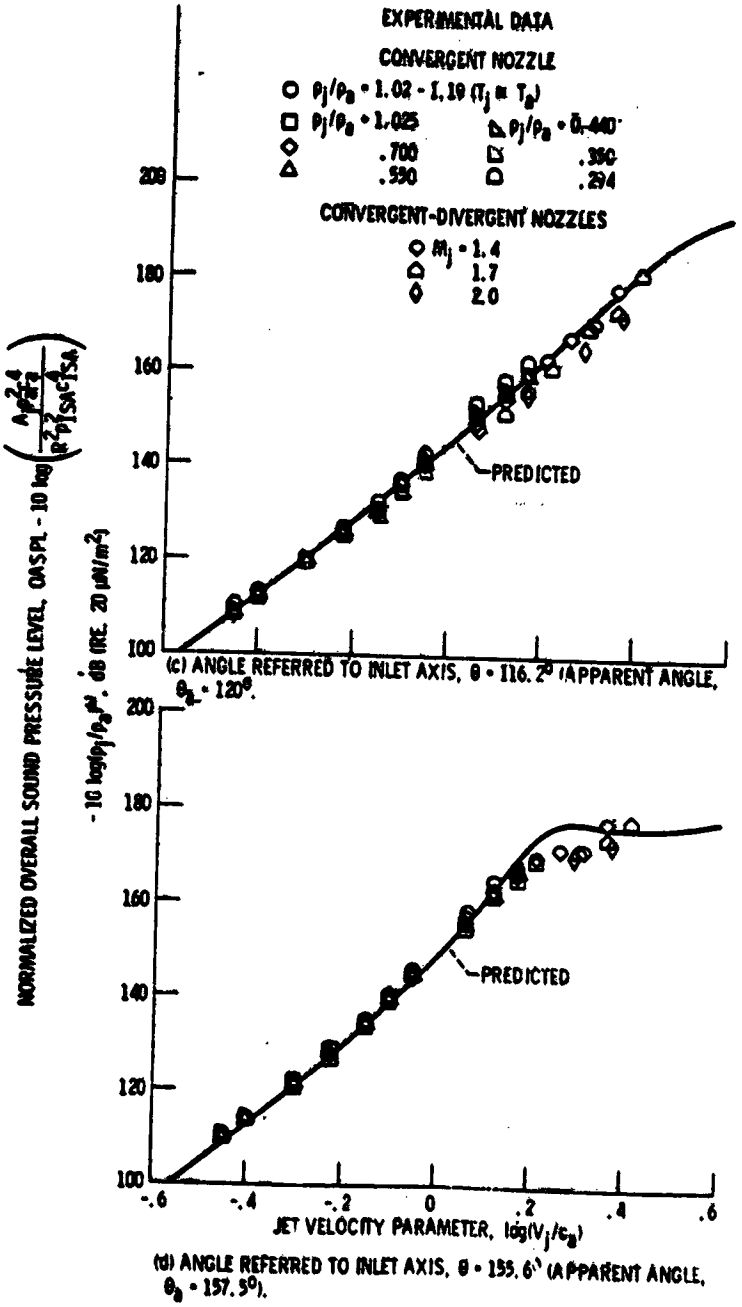

Figure 6. - Concluded.

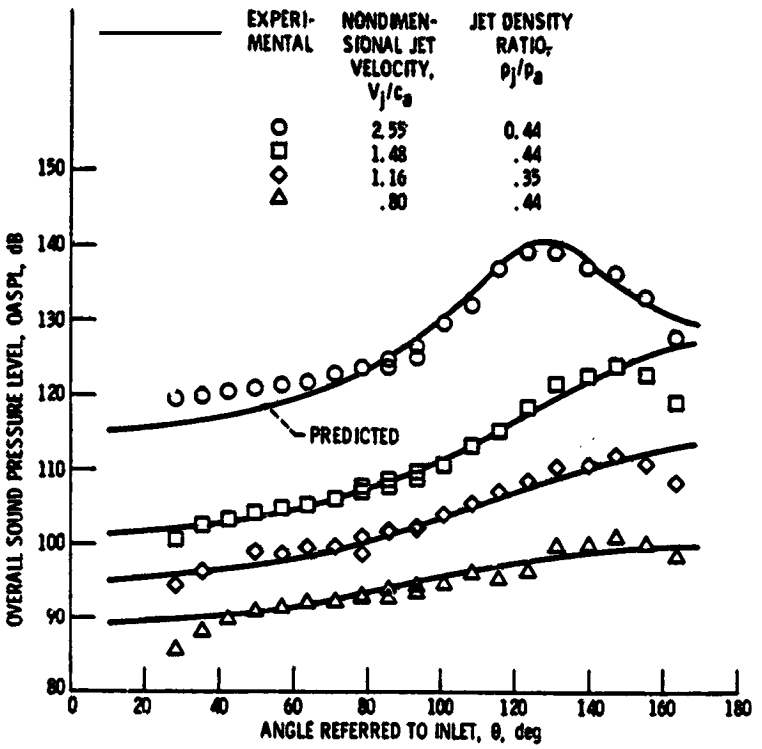

Figure 7. - Comparison of static jet mixing noise prediction with experimental directivity data of Tanna, et al. (ref. 16) for 5.08-cm-diameter nozzles.

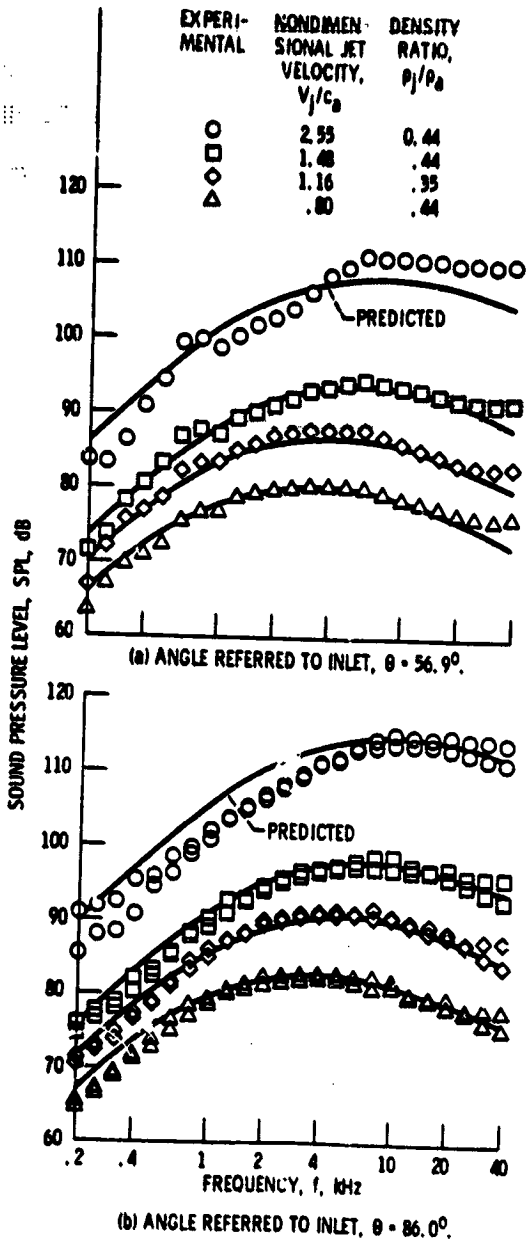

Figure 8. - Comparison of static jet mixing noise prediction with experimental 1/3-octave-band spectra of Tanna, et al. (ref. 16) for 5.08-cm-diameter noz-

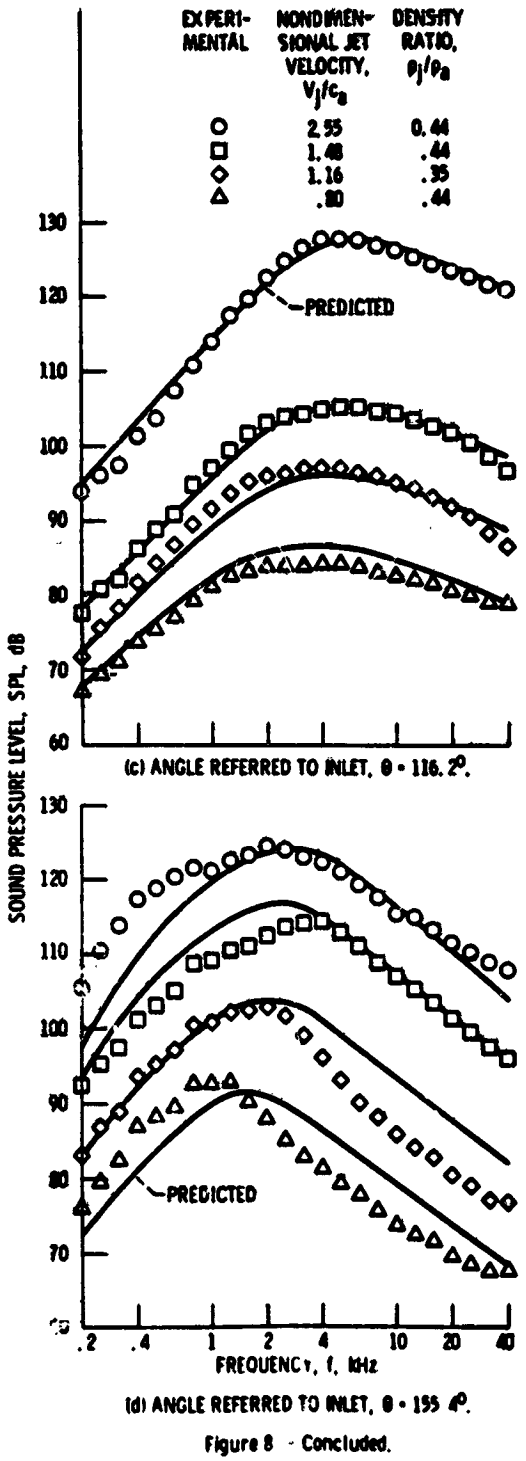

(c) ANGLE REFERRED TO INLET, $\theta = 116.2^{\circ}$.

(d) ANGLE REFERRED TO INLET, $\theta = 155.4^{\circ}$.

Figure 8 - Concluded.

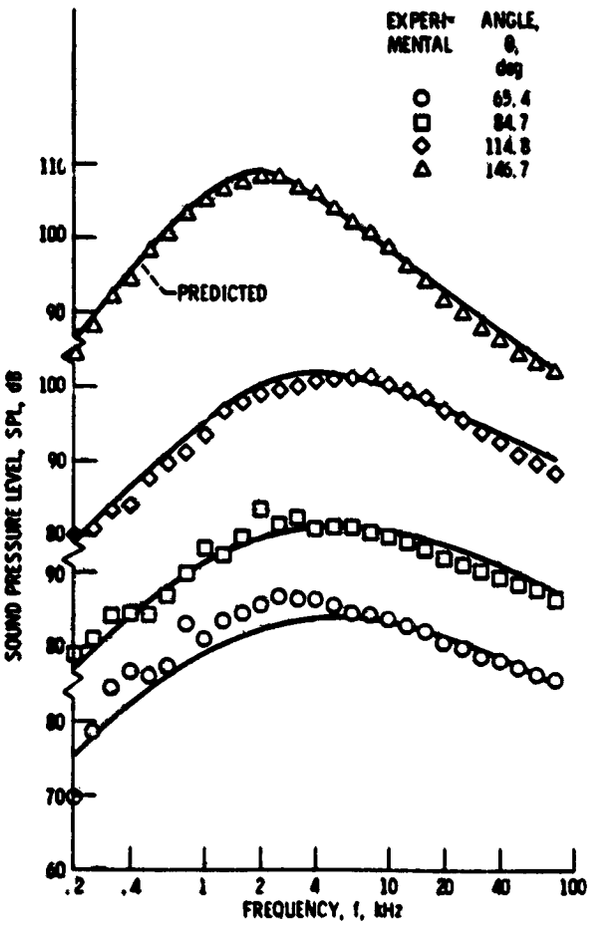

Figure 9. - Comparison of flight jet mixing noise prediction with simulated flight data of Kozlowski and Packman (ref. 17) for 5.7-cm-diameter nozzle in free jet at free jet Mach number, $M_0 = 0.18$, and nondimensional jet velocity, $V_j/c_a = 1.38$.

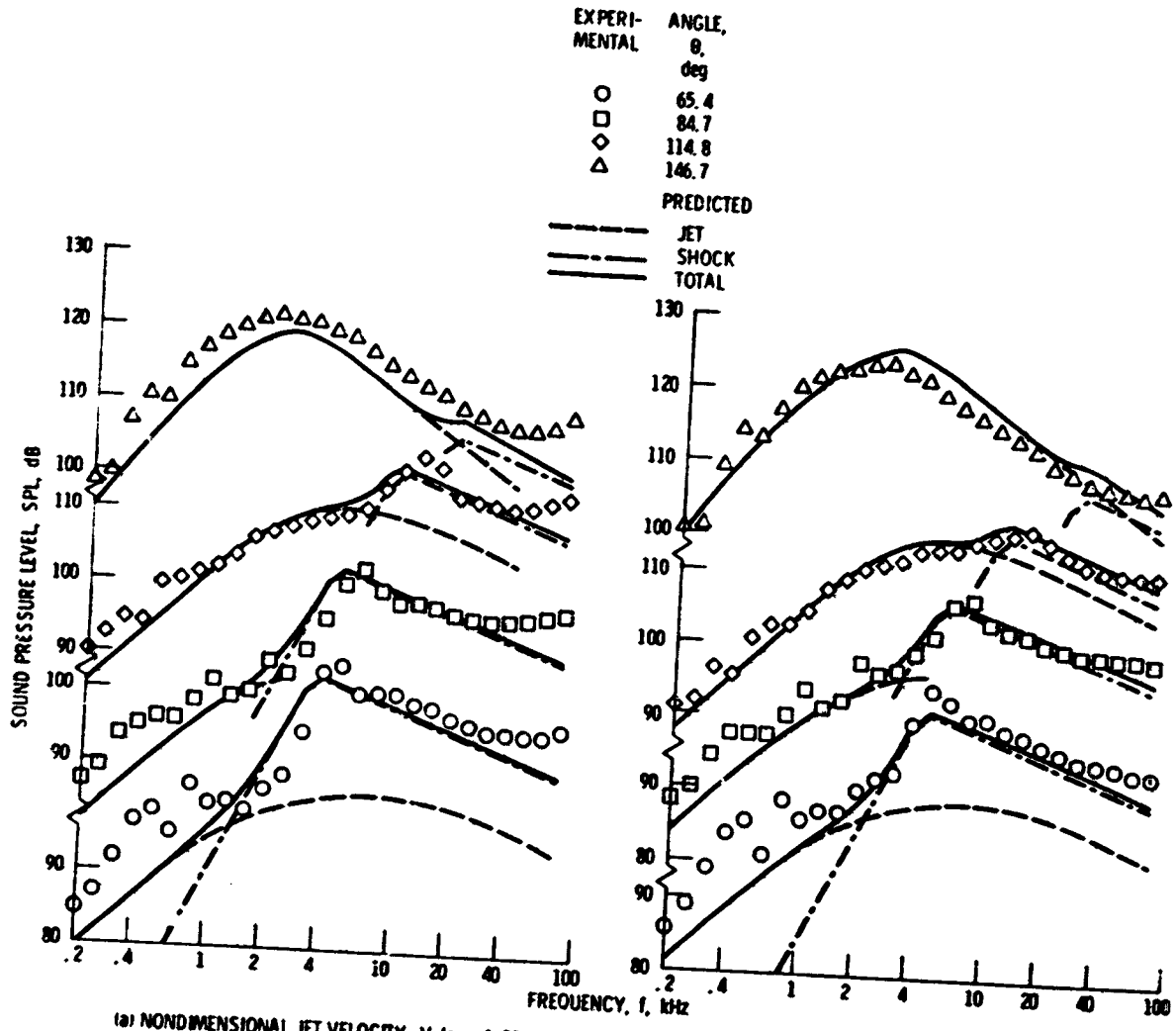

Figure 10. - Comparison of static shock and jet mixing noise prediction with data of Koziowski and Parkman (ref. 17) for a 5.7-cm-diameter nozzle at jet Mach number, M_j = 1.41.

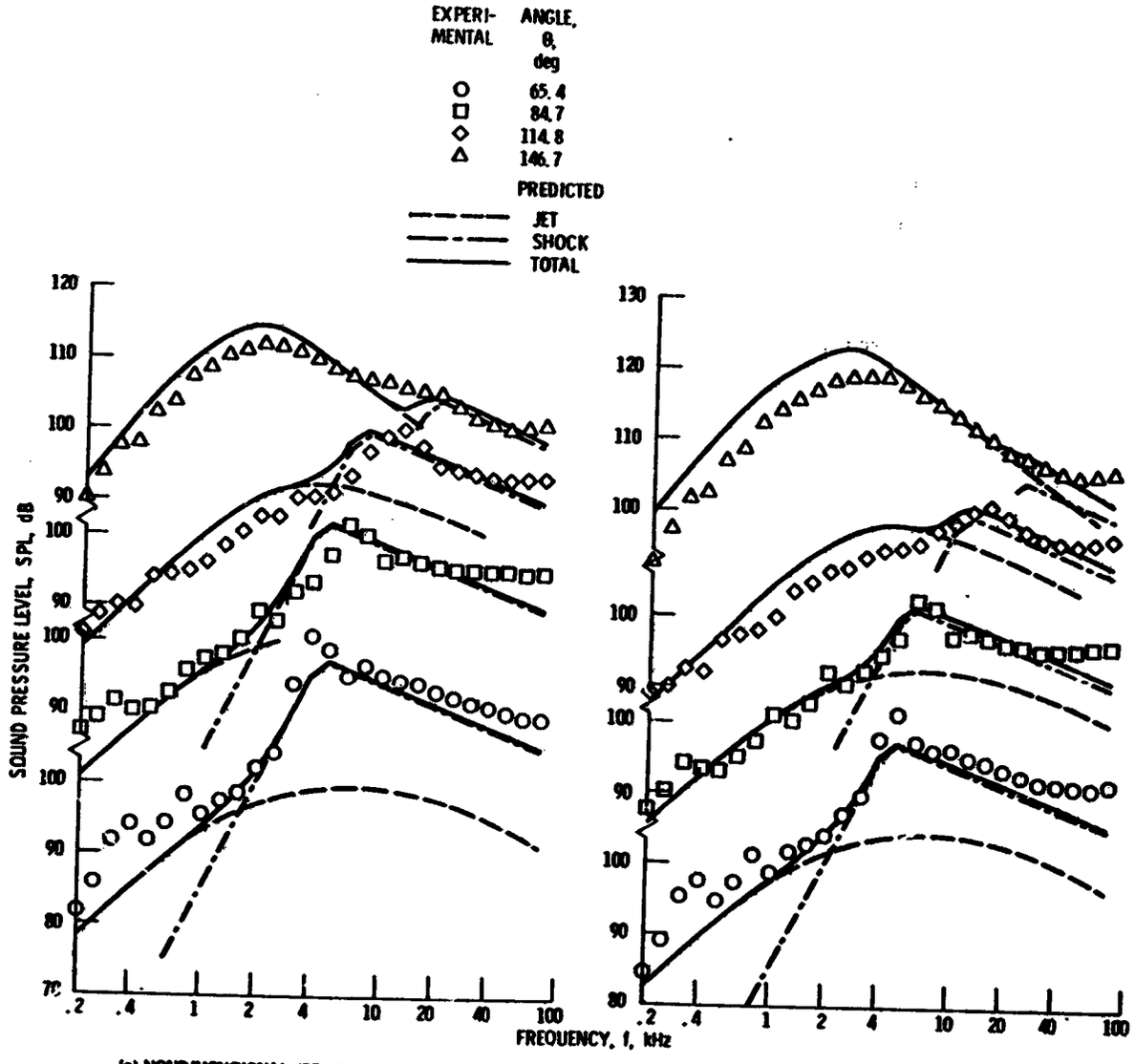

Figure 11. - Comparison of shock and jet mixing noise prediction with data of Kozlowski and Packman (ref. 17) for a 5.7-cm-diameter nozzle at jet Mach number, M_j = 1.41, and free-jet Mach number, M_0 = 0.18.

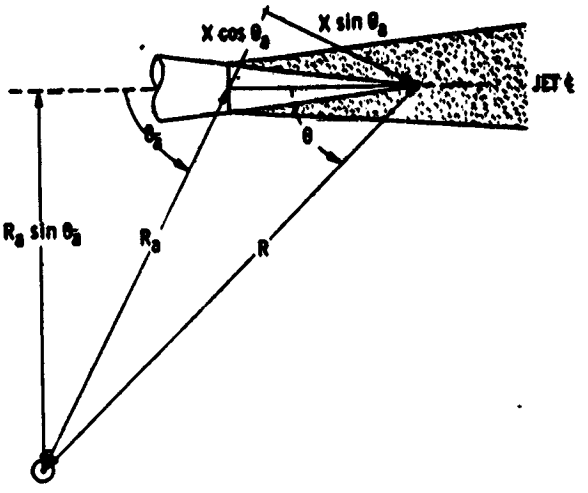

Figure A1. - Geometric relations for jet noise source located downstream of nozzle exit plane.

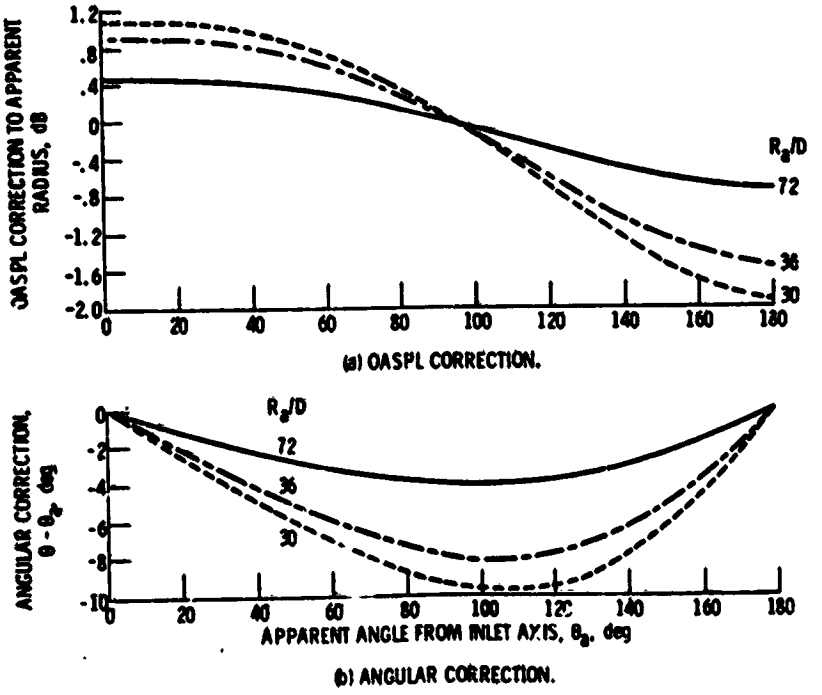

Figure A2. - Corrections to be applied to jet noise data taken at constant apparent radius.